SHORT TAKEOFF OPTIMIZATION FOR THE XV-15 TILTROTOR AIRCRAFT

T.M. Cerbe
Lufthansa German Airlines, Hamburg, FRG
G. Reichert
Technical University of Braunschweig, FRG
D.P. Schrage
Georgia Intitute of Technology, Atlanta, USA

Abstract

Tiltrotor aircraft are being developed for a variety of military and civil operations. Although a tiltrotor aircraft will often make use of vertical takeoff, the short takeoff is of importance for some applications under specific conditions, such as high gross weights or unfavorable ambient conditions. Whereas the vertical takeoff is well understood due to its similarity to the vertical takeoff of conventional helicopters, there is a lack of information about how to perform the best short takeoff procedure. The short takeoff performance and the short takeoff distance depend on many variables. Few, if any, studies have investigated the calculation or the optimization of the short takeoff for tiltrotor aircraft. Most often, the estimation of short takeoff performance has been based on the experience gained from XV-15 tiltrotor aircraft flight tests. These flight tests, however, utilized only a fixed nacelle tilt angle and a fixed wing flap deflection.

Considerable research in the Federal Republic of Germany (FRG), specifically at the Technical University of Braunschweig, has been ongoing for the past five years to investigate optimization methods for airplane and helicopter takeoff and landing. This research has been sponsored as part of a broad program by the FRG government to address "Sicherheit im Luftverkehr" (Safety in Flight) issues. This research utilizes simulation models validated with flight test data and coupled with numerical optimization methods. As part of a collaboration effort between the Technical University of Braunschweig and the Georgia Institute of Technology, these methods have been extended to investigate short takeoff optimization for the XV-15 tiltrotor aircraft.

The main objective of this effort was to provide more information about the short takeoff capability of civil tiltrotor aircraft. This information is helpful for the design of new tiltrotor aircraft, the development and construction of new vertiports, and the specification of One-Engine-Inoperative (OEI) requirements. In addition, the FAA could use additional short takeoff data to review the new criteria for civil tiltrotor aircraft. Since the short takeoff depends on many variables, such as gross weight, ambient conditions, power available, flap setting, nacelle tilt, and maneuver strategy, takeoff related performance is analyzed by varying different parameters. The takeoff distance is minimized using the optimization methods developed at the Technical University of Braunschweig. The takeoff simulation is carried out using the Generic Tilt Rotor Simulation (GTRS). The XV-15 geometric and aerodynamic data sets are used. Because GTRS has never been consistently correlated with XV-15 flight test data for the low-speed flight region OGE and IGE, which is relevant for the short takeoff, the aerodynamic modeling for horizontal speeds less than 60 knots must be proven. Therefore, a further objective of this effort was to develop a more reliable simulation model.

The results of this investigation will be presented as well as the recommended changes to the GTRS model necessary for short takeoff optimization for tiltrotor aircraft.

Notation

B	Tip Loss Factor
c	Constant
c_D	Drag Coefficient
c_P	Power Coefficient
c_T	Thrust Coefficient
c_W	Weight Coefficient
D	Rotor Diameter
DL	Download
F	Cost Function
FB	Brake Force

FN1, FN2	Nose, and Main Gear Vertical (Normal)Force
G,GW	Gross Weight
GECON1	Ground Effect Constant
GECON2	Ground Effect Constant
GEWASH	Ground Effect Washout Factor
H	Rotor Height above Ground
H1	Takeoff Decision Height
I_{yy}	Moment of Inertia, Y-Axis
N_{MG},N_{NG}	Normal Force of Main and Nose Gear in Ground Axis System
m	Aircraft Mass
M_i	Pitch Moments of Aircraft Subsystems
M_G	Landing Gear Moment
PREQ	Power Required
q	Pitch Rate
QREQ	Torque Required
R	Rotor Radius
t	Simulation Time
Ui	Optimization Parameter
V	True Airspeed
V1	Takeoff Decision Speed
V2	Takeoff Safety Speed
VEF	Speed at Engine Failure
VLOF	Lift-off Speed
VROT	Rotation Speed
u	Longitudinal Velocity
v	Lateral Velocity
w	Vertical Velocity (Rate of Climb/Descent)
w_i	Rotor-Induced Velocity
w_{iH}	Rotor-Induced Velocity in Hover
x	Takeoff Distance
X_B	Brake Force
X_i,Z_i	Forces of Aircraft Subsystems
XCOL	Collective Control Input
X_G	Landing Gear X-Forces
XLN	Longitudinal Control Input
Z_G	Landing Gear Z-Force
α	Angle of Attack
δ_i	Profile Drag Coefficients of Rotor Blades
κ	Non-Dimensional Climb Speed
λ	Non-Dimensional Axial Flow
μ	Non-Dimensional Forward Speed
μ_B	Brake Force Coefficient
μ_R	Rolling Friction Coefficient
Ω	Rotor Speed
Θ	Euler Pitch Angle
AEI	All Engines Operating
CDP	Critical Decision Point
CTR	Civil Tilt Rotor
EUROFAR	European Future Advanced Rotorcraft
FAA	Federal Aviation Administration
GARTEUR	Group for Aeronautical Research and Technology in Europe
GTRS	Generic Tilt Rotor Simulation
IGE	In Ground Effect
NASA	National Aeronautics and Space Administration
OEI	One Engine Inoperative
OGE	Out Ground Effect
PDP	Power Deficiency Parameter
SCAS	Stability and Control Augmentation System
S.D.	Standard Day
S.L.	Sea Level
STI	Systems Technology Incorporation
VMS	Vertical Motion Simulator

1. Introduction

The concept of the tilt rotor aircraft has been an on-going research effort in the United States since the early 1930's, when the first tilt rotor patents were filed, Ref.1. One major step in the evolution of the tilt rotor aircraft was the development and construction of the XV-15 research aircraft in the 1970's by Bell under a NASA-Army contact, Ref. 2. The first flight took place on May 3, 1977. Extensive ground and flight testing of this aircraft, conducted from 1977 through 1983, are well documented in Ref. 3. In the late 80's Bell and Boeing helicopter companies constructed the V-22 Osprey, a military fullscale development program, under contract to the U.S. Navy.

The V-22 made its first flight in March 1989, Ref. 4. Civil tilt rotor design studies are underway in the United States, Europe, and Japan to meet the prospective requirements of future commercial markets, Refs. 5 to 9. In the United States, five different candidates for a civil tilt rotor (CTR) aircraft ranging from an 8-passenger executive to a 75-passenger transport were investigated, Ref. 6. In Europe, a collaborative study has been conducted by the Group for Aeronautical Research and Technology in Europe (GARTEUR) to access the applicability of tilt rotor aircraft and compound helicopters to civil missions, Ref. 7. The study provided a justification for launching the first phase of investigations on the European Future Advanced Rotorcraft (EUROFAR), a 30-passenger tilt rotor aircraft. The EUROFAR design is described in more detail in Ref. 8. Suggestions on how to enable the next generation of tilt rotor aircraft to achieve higher forward velocities than today's tilt rotor designs are presented in Ref. 9.

The helicopter industry and NASA have proven through extensive flight testing that the tilt rotor concept is feasible from the technical standpoint. However, the success of a civil tilt rotor mainly depends on the development of the required infrastructure, Ref. 10, and the public acceptance. Although tilt rotor aircraft can land and operate from existing airports and heliports, they also must have their own operating sites in order to be truly effective. These vertiports must include vertical landing spots and should have a short takeoff area to enable takeoffs at higher gross weight with more payload. Regarding the public acceptance, besides the travel costs, the safety of the tilt rotor aircraft during all operations is of major importance. Takeoff and landing are the most critical flight phases. The takeoff criteria must be carefully determined and used in sizing a civil tilt rotor configuration to meet safety requirements.

Surveys showed, Ref. 5, that an one engine inoperative (OEI) hover out of ground effect (OGE) capability for the vertical takeoff is needed. In the event of an engine failure during takeoff, the takeoff can continue at any time. The OEI hover capability is one important factor in determining engine power requirements. Alternatively, the power deficiency parameter (PDP) could be used as design criterion. If the PDP is grater than zero but small (no OEI hover capability OGE), vertical takeoff procedures for conventional helicopters, which are characterized by the critical decisions point (CDP), must be applied to the civil tilt rotor aircraft. In this case, a certain takeoff area is required either to continue takeoff and clear a 35-ft obstacle or to reject takeoff and land safely. For a high PDP (high gross weight) where even the hover flight in ground effect (IGE) can not be carried out, the short takeoff procedure must be applied. Currently, the estimation of short takeoff performance is based on the experience gained from XV-15 flight tests, Ref. 3 and 11.

2. Short Takeoff Procedure

According to the Interim Airworthiness Criteria for Powered-Lift Category Aircraft, Ref. 12, the takeoff distance is defined as a greater distance of either: the horizontal distance taken to attain and remain at least 35 ft above the takeoff surface with a speed of at least V2 and a positve rate of climb when the critical engine fails at VEF, or: 1.15 times the horizontal distance along the takeoff path without engine failure. This path is measured from the starting point of the takeoff to the point at which the aircraft attains and remains at least 35 ft above the takeoff surface. Figure 1 shows the short takeoff procedure for a tilt rotor aircraft.

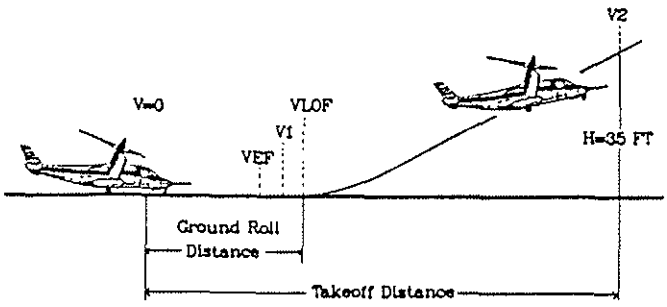

Figure 1 Short Takeoff Flight Path

VEF is the speed at which the critical engine failure occurs, and V2 is the takeoff safety speed at which a safe climb is assured. For any given set of conditions (such as weight, configuration, ambient conditions and wind), a single takeoff decision point and a single value of V2 must be used. The takeoff decision point is the point where, in the case of a single engine failure at VEF, the aircraft can be either stopped safely on the takeoff area (rejected takeoff) or continued. The takeoff decision point must be established as a single parameter such as speed, V1, or a combination of no more than two suitable parameters, such as speed, V1, and height, H1.

The rejected takeoff distance is defined as the distance between the starting point and the point where the aircraft comes to a full stop. The rejected takeoff distance must be established with and without engine failure. A time delay of 2 sec after reaching V1 has to be accounted for, before the pilot applies means of rejecting the takeoff. The lift-off speed VLOF is determined mainly by the requirement for the OEI climb performance, which requires a steady gradient of climb not less than the greater of 1.7 % or 150 ft/min at VLOF for two-engine aircraft. The ground effect can be taken into account. With the landing gear retracted, the steady gradient of climb OGE must not be less than the greater of 2.4 % or 200 ft/min at V2 for two-engine aircraft. All flight reference speeds, such as VLOF, V1, and V2 depend on gross weight, ambient conditions, and engine power available.

Short takeoff flight testing with the XV-15 was performed by NASA Ames in 1982, Ref. 11, for a gross weight of 15000 lbs. Takeoffs were made with 20 deg nacelle tilt angle, 40 deg wing flap deflection, 98 % RPM, and approximately 80000 in-lbs mast torque per rotor. The value for the mast torque represents single engine contingency power based on transmission limitations so that the results presented in Figure 2 demonstrate the OEI performance of the XV-15. Takeoffs were made at lift-off speeds from 25 to 55 kts. The pilot's takeoff technique was as follows: set longitudinal cyclic trim at 50 %; set nacelles at 20 deg; increase power to 45000 - 50000 in-lbs mast torque; release brakes; pull power in smartly to desired value (80000 in lbs); rotate the aircraft and adjust pitch attitude in order to hold desired airspeed through 50 ft radar altitude. The stability and control augmentation system (SCAS) including rate feedback but without attitude hold mode was used. Figure 2 shows the final results from Ref. 11.

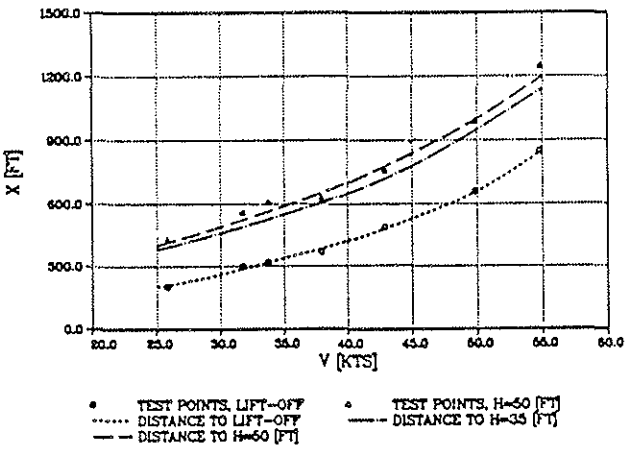

Figure 2 Takeoff Distance from XV-15 Flight Tests

The figure presents the ground roll distance and the total takeoff distance to clear the 50 ft altitude versus lift-off speed. In addition, the distance to clear 35 ft altitude is shown. As one would expect, the takeoff distance increases with higher lift-off speeds. This increase is mainly due to an increasing ground roll distance, i.e. the distance from the starting point to the point where the aircraft is airborne. The distance required to climb to 50 ft attitude increases only slightly.

Figure 3 shows the time histories. The takeoff at a lift-off speed of 30 kts is chosen from Ref. 11. The control speed for the collective control input reaches an average value of 5 %/sec. The values for the longitudinal cylic input are of the magnitude of 10 %/sec. The maximal pitch attitude during the takeoff is in all cases (not shown here) about 20 deg or less. The rotation phase begins where the longitudinal control input changes and the pitch angle increases. At the same time the nose gear becomes free. About 2 sec more are required until the main gear is free and the aircraft is airborne. The roll distance to the point where the pilot initiates the rotation is about 120 ft. The airspeed at this time is somewhere between 20 and 30 kts. The additional distance until the aircraft is airborne is about 110 ft. Although the pilot was asked to hold the desired airspeed, in most cases, the airspeed is decreasing slightly after reaching a maximum value (also see pitch angle). Note that the torque increases above the value of 80000 in-lbs per rotor. Experience from these flight tests was used to set up the takeoff procedure for the flight manual of the XV-15, Ref. 17. The flight manual recommends a nacelle tilt angle between 0 and 20 deg and a flap position of 40 deg.

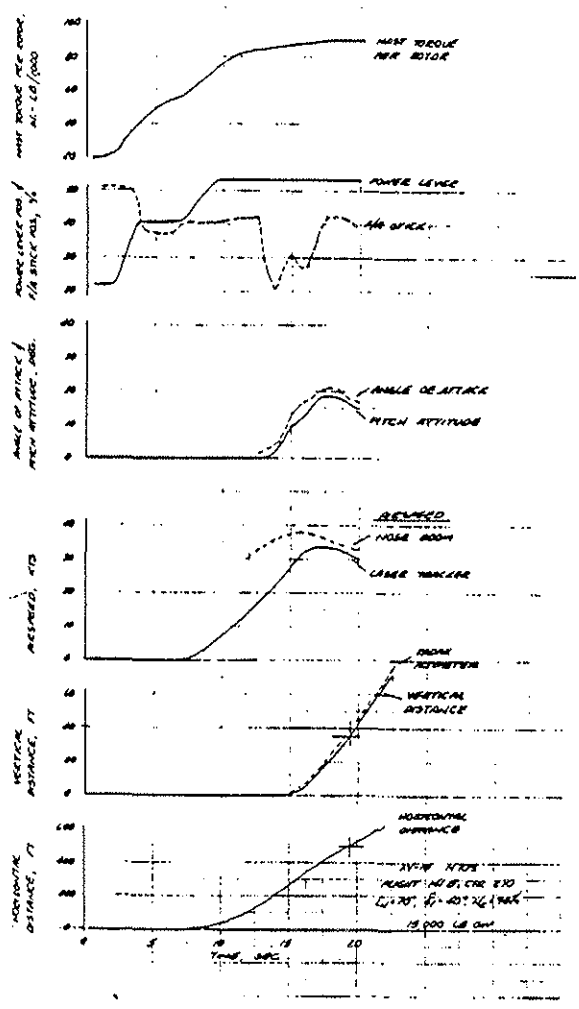

Figure 3 XV-15 Takeoff from Flight Tests

The flight test results can be used for qualitative comparison. For a quantitative comparison with simulation results, the conrol input histories would be needed in digital form to use as input data for the takeoff simulation. In addition, the takeoff flight tests were performed under wind conditions with winds between 5 and 9 kts, but the wind velocities were not recorded. Since wind velocities of this magnitude influence the takeoff distance, takeoff flight testing in general should be carried out under zero wind conditions or winds less than 1 kt, if no wind recording is available. However, some information for the simulation task can be extracted from the flight test results.

For the simulation, the SCAS including the attitude mode is used to stabilize the aircraft in the phugoid mode. As mentioned above, the attitude hold mode of the SCAS was not used during the flight tests. Therefore, the longitudinal control inputs required for the simulation will be different from the control inputs shown in Figure 3.

During the rolling phase the longitudinal control input is set to 50 %. The collective control is increased with a steady gradient of 5 %/sec until the maximum torque of 85000 in-lbs per rotor is reached. After this, the collective is kept constant. A maximum torque of 85000 in-lbs instead of 80000 in-lbs was chosen, since the average flight test value was of this magnitude. The initial value for the collective at the time t=0 sec is chosen in such a way that the aircraft does not start to roll *(the maximum brake force is used)*.

The flap position and the nacelle tilt angle are set in the beginning and are not changed during the takeoff. A variable control of the flap position and the nacelle tilt angle could be of advantage for an optimal takeoff decreasing the takeoff distance, but would considerably increase the pilot workload. The longitudinal input is variable in order to control the takeoff flight path.

3. Simulation and Optimization Model

Generic Tilt Rotor Simulation

The simulation model used in this study is the Generic Tilt Rotor Simulation (GTRS), Refs. 15 and 16. The original version was developed by Bell for the XV-15 research aircraft. A generic real-time version of this model for use on the vertical motion simulator (VMS) at NASA Ames was developed by Systems Technology Inc. (STI). The first release of this development was completed in 1983. A version of the simulation code including input data sets for the XV-15 were provided to the School of Aerospace Engineering, Georgia Insitute of Technology, where the model was implemented on a VAX 11/750. A complete description of the mathematical model can be found in Ref. 16. Here, only some features related to the takeoff simulation will be addressed. Validation of the GTRS through the use of XV-15 flight and wind tunnel tests was accomplished and documented by STI, Ref. 18.

The GTRS model is a well structured code written in FORTRAN. The source code includes the main program and more than 60 subroutines, containing the mathematical model for the different aircraft components, such as the two rotors, the fuselage, the wing, the horizontal and vertical stabilizers, the landing gear, the two engines and the drive system, the rotor collective governor, and the SCAS. In addition to the main input data, 304 input data tables are used to provide information, such as the aerodynamic coefficients for the different aircraft components, the interactional aerodynamics between rotor/wing/fuselage/stabilizers/ground, the gains and coefficients for the control system, etc.. The aerodynamic data in these tables are derived mainly from wind tunnel tests. The control input histories, which are necessary to "fly" the simulation model are part of the main input data deck. Different kinds of control histories, such as step and sines/cosines functions, can be chosen.

The mathematical model of the rotor is based on the theory in Refs. 19 and 20 except that it is derived in the mast-axis system and contains provisions for prop-rotor characterics such as nonlinear twist, flapping restraint, and pitch-flap coupling. Rotor flapping forces and moments are calculated in the "wind-mast" axis system and are transformed into the mast-axis system. The rotor-induced velocity is computed by calculating the induced velocity of an isolated rotor OGE, and then modified to account for the side-by-side rotor effect, the tandem rotor effect in sideward flight, and the ground effect. The value of the isolated rotor-induced velocity OGE is approximated using a modified expression from Ref. 21. This expresion contains a correction of the momentum theory equation to avoid the singularity in the vortex ring region. The major

assumptions made with regard to the induced velocity is that it is uniform over the rotor disc.

First trim results with GTRS for hover and forward flight OGE showed that calculated power required in the low speed region increased above hover power required before decreasing with forward speed. Since this result was different from typical power required curves known from conventional helicopters and could not be explained by secondary effects, e.g. download changes with forward speed, an error in the induced velocity equation was suspected. Evaluation of the equation in the code and comparisons with the original equation from Ref. 21 led to the following equation for the rotor-induced velocity:

$$w_i = \frac{\Omega R c}{\sqrt{0.866\lambda^2 + \mu^2}\,\frac{0.6|c|^{1.5}\left(|c| - \frac{8}{3}\lambda|\lambda|\right)}{\left(|c| + 8\mu^2\right)\left(|c| + 8\lambda^2\right)}} \qquad (3.1)$$

with:

$$c = \frac{c_T}{2B^2} \qquad \lambda = \frac{w_i}{\Omega R} \qquad B = 0.97$$

The correction changed the power required curve in the low speed region dramatically, thus additional changes to GTRS input data were required. After informing STI and Bell the profile drag coefficients for the rotor blades and the wing-pylon drag coefficients were modified to adjust power required and download to flight test results. The new profile drag coefficients are:

$\delta_0 = 0.013$	$\delta_1 = -0.100$	$\delta_2 = 0.58$	new values
(0.015)	(-0.068)	(0.81)	old values

These coefficients are used in the profile drag equation, along with the angle of attack:

$$c_D = \delta_0 + \delta_1 \alpha_R + \delta_2 \alpha_R^2 \qquad (3.2)$$

The wing-pylon drag coefficients have been corrected for angles of attack in the region of -90 deg. The correction was necessary to match the download from flight tests in the order of 13.7 % for a flap position of 40 deg. This value was taken from Ref. 3, Vol. 2. The download of the original GTRS was 12.7 %. The new drag coefficients are shown as a function of the angle of attack for different flap settings in Figure 4.

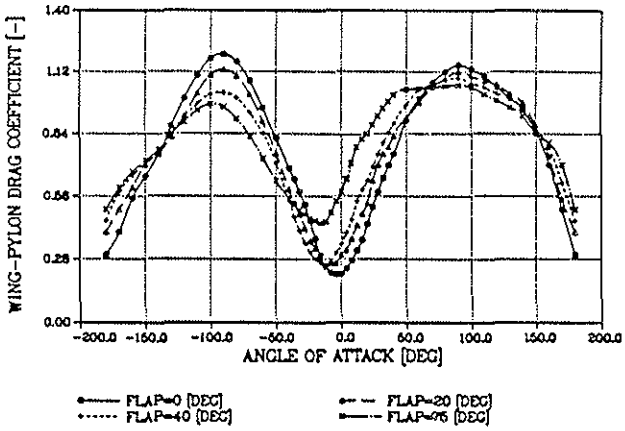

Figure 4 Wing-Pylon Drag Coefficients versus Wing Angle of Attack

The reduction in the induced velocity caused by ground effect is calculated using an exponential expression. This expression is derived from Ref. 22, which gives an empirical relation for the ground effect in hover flight. It has been shown in Ref. 18 that although this relation was derived from flight tests of conventional helicopters, it can be adjusted to the XV-15 flight test results IGE. At forward speeds of about 30 kts the ground effect is washed out. The influence of forward speed on the induced velocity IGE is described by an exponential function:

$$\Delta w_{i,IGE} = w_{i,OGE}\left[1 + (G - 1)e^{\dot{W}}\right] \qquad (3.3)$$

with: $G = 1 - \text{GECON}\,1e^{\text{GECON}2\left(\frac{H}{2R}\right)}$

and $\dot{W} = \text{GEWASH}\sqrt{(u^2 + v^2)}$

The factor GEWASH in this equation was changed from -0.08 to -0.04, since it was found that the increase of power required for speeds between 0 and 30 kts was too strong. Flight tests with the helicopter BO 105, Ref. 23, have shown that power required increases only slightly over hover power required IGE with forward speed.

The GTRS version delivered to Georgia Tech did not include a model for the dynamics of the landing

gear. It consisted only of the calculation of landing gear drag and landing gear pod drag based on wind tunnel measurements. Because existing landing gear models for the XV-15 used in the real-time simulation at NASA Ames showed landing gear modelling instabilities and no other landing gear model was available, a simple rigid landing gear was developed and added to GTRS.

The new landing gear model takes into account the gear normal forces, the gear drag forces due to friction, the brake force, and the resulting pitching moment of the nose and the main gear. Since in this study no asymmetrical trim states or maneuvers are considered (zero wind condition), the side forces as well as gear and roll moments are not included. The stiffness of the landing gear is assumed to be infinite, thus the gear normal forces can be calculated directly, instead of first calculating the stroke rates in case of a dynamic landing gear. The major assumption is that the landing gear oleo strokes for the rolling takeoff are small and have a negligible effect on pitch angle changes and thus changes of angle of attack during the rolling phase. Estimation of the pitch angle for a flexible landing gear model showed values less than 1 deg. The pith angle during the rolling phase is assumed to be constant and equal to 0 deg. Details of the landing gear model can be found in Ref. 24.

Two different SCAS models were developed, one by Bell and one by NASA. However, only the NASA-developed SCAS is available for use in the GTRS-version. Besides the SCAS model, the rotor collective governor, the engines, the fuel control, and the drive system dynamics is modeled. In this study, the engine turbine NII governor is used as an overspeed governor. The governor will act, if 104 % RPM are exceeded. As a result, the rotor speed increases slightly for increasing collective control input. The overspeed is less than 2 % for all simulated takeoffs, because the rotor collective governor reduces collective pitch, if rotor speed increases.

Takeoff maneuvers are considered as relative "slow" maneuvers within the lower frequency range. Therefore, a simulation step size of 0.1 sec instead of the 0.01 sec can be used in order to reduce computation time. Comparative simulations have shown a negligible computational error.

Optimization Method

For the optimization problem in this study a numerical method is applied, which is available as a FORTRAN subroutine called EXTREM, Ref. 13. The code EXTREM can be used for the determination of a local optimum of a multi-variable cost function without knowledge of its analytical derivations. The optimal parameters, leading to an optimal function value (minimum or maximum), are calculated by means of systematical variation of the parameters and the search direction. Constraints of all kinds can be taken into account. As an example, Figure 5 shows the proceeding of EXTREM for a three-dimensional problem, i.e., a cost function that only depends on two parameters U1, and U2.

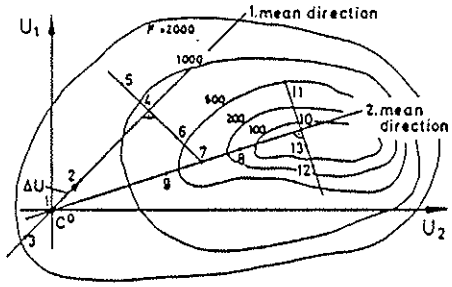

Figure 5 Principle Optimization Method of EXTREM

Based on the initial values for U1, and U2, the cost function F is calculated in points 1 (estimated value), 2, and 3 (each being a search step of the first main search direction). A parabolic extrapolation yields point 4. This point is the optimum of a parabola through points 1 to 3. By means of a Gram-Schmidt orthogonalization, the first secondary search direction and the extreme value 7 are determined. The second main search direction always results from connecting the optimum of the last and the next to the last secondary search direction. Accordingly, the third main search direction would result from points 7 and 13. For the three-dimensional example with two parameters, the optimization strategy is representable. With an increasing number of optimization parameters, the computation time increases. Basically, the number of parameters should be only as high as the optimization problem requires. A number too low may restrict the possible solutions of a problem.

Normally, complex multi-dimensional functions have several local optima. The search for the global optimum can be improved by predetermining different

combinations of estimated initial values. This task can be taken on by the program GLOBEX, Ref. 14, which determines initial values for the optimization parameters by means of normally distributed random numbers. Figure 6 shows the simplified optimization structure.

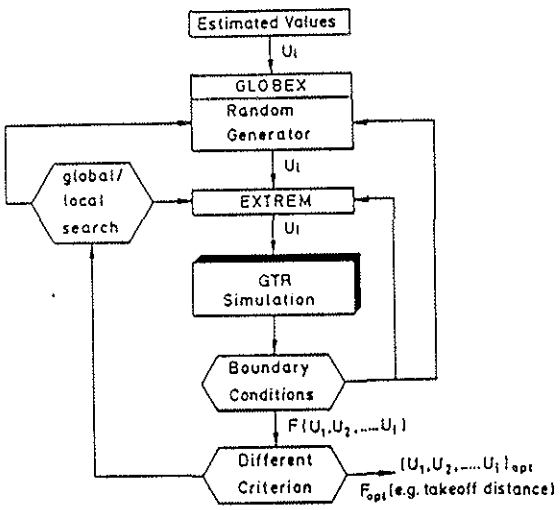

Figure 6 Optimization Structure including the GTRS model

The precondition for optimization with EXTREM is the knowledge of initial values for the optimization parameters, which do not violate the given constraints. The search for permitted initial values can be taken on by GLOBEX as well, before three overriding optimization segments are initiated. Each optimization segment is subdivided into several subsegments, which in turn consist of several optimization steps. Each optimization step comprises the calculation of the cost function, i.e., a complete takeoff simulation. Interruption of the optimization is possible on the basis of different criteria, as there are a minimum change of the optimal cost function value, a minimum change in the optimization parameter, or simply the number of optimization segments.

For the short takeoff requiring a minimum takeoff distance, the maximum power available should be used. Also, the increase in power per unit time should be as high as possible. Therefore, the collective control input is given and does not vary during the optimization. The only variable control input during the takeoff simulation, which can be changed by the optimization algorithm, is the longitudinal control, i.e. the longitudinal stick position. The longitudinal stick position is coupled with the longitudinal cyclic input to the rotors and with the elevator deflection. Both can not be varied independently. Figure 7 shows a typical time history for the longitudinal control.

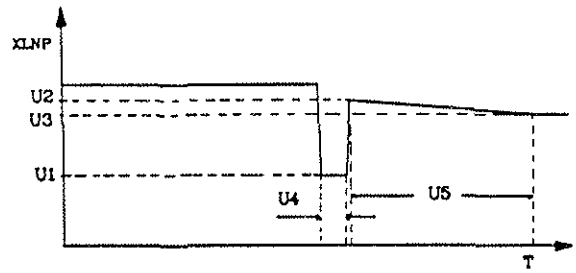

Figure 7 Longitudinal Stick Position versus Time

There are only five optimization parameters U1...U5 to represent the longitudinal control. It was decided to use this simple control function in order to keep the number of parameters as low as possible. In addition to these parameters, the switching time, at which the rotation is initiated, is variable. The forward speed is chosen as the criterion to start the rotation. If a certain forward speed is reached, the longitudinal control changes from the 50 % position to the desired value U1.

In some optimization runs, the wing flap deflection and the nacelle tilt angle are optimization parameters. Since these parameters are constant during the takeoff, the optimization task can be solved in two steps. In the first step, optimization runs are performed, in which flap deflection and tilt angle are given, and the optimal longitudinal control input is found for one flap/tilt configuration. After finding the optimum takeoff for selected configurations, further optimization runs are started based on the first results. The main reason for this procedure is that the second step requires considerably more computation time because of additional optimization parameters, and because a trim calculation has to be carried out before each simulation. (As will be shown in Figures 21 to 23, the ground trim depends mainly on the nacelle tilt angle). In contrast, the first step needs just one trim calculation before the optimization starts, since all following takeoff simulations begin with the same trim conditions. This way, computation time has been reduced. The longitudinal control input is limited by the minimum and maximum stick position varying from 0 to 100 %. For the wing flap deflection there are four positions available in

the XV-15: these are 0, 20, 40, and 75 deg. Flap positions of 40 and 75 deg are the most interesting ones. The nacelle tilt angle is limited to values between -5 and 30 deg. A minimum value of 10 deg has been investigated. A nacelle tilt higher than 30 deg can not be used for geometric reasons. The rotors would have ground contact for small roll angles. Further constraints result from aerodynamic limitations, as there are, rotor endurance limit, and wing stall. The last constraint is imposed by a requirement related to the passenger comfort. Vertical accelerations higher than 1.15 g are not allowed. If one of these limits is reached during the takeoff simulation, the takeoff is terminated, and the next takeoff with new optimization parameters is initiated.

The cost function is comprised mainly of the takeoff distance. The optimization task is the minimization of the takeoff distance. The takeoff distance is the distance from the starting point to the point where the aircraft clears a 35 ft obstacle. To prevent exotic takeoff maneuvers, e.g. strong and continuous pull up maneuvers to gain height in favor of speed, certain horizontal and vertical speeds have to be reached. These final speeds can either be given before the optimization, or can be selected during the optimization. If the speed is selected during the optimization, the horizontal and vertical speeds are averaged over the time needed to climb from the 35 ft height to a height of 100 ft. The cost function contains the quadratic error between the actual speed and either the average speed or the given speed integrated over a time interval.

4. Simulation Results

Takeoff distance depends mainly on power required and power available. Therefore, a reliable calculation of power required and power available is important for takeoff simulations. The present study is more concerned with the aerodynamic modelling of the aircraft and the calculation of power required, whereas the available power is assumed to be calculated accurately by the given engine model. Since the takeoff is performed inside the low speed flight regime, the discussion of power required curves is limited to hover flight and forward speeds up to 70 kts. The minimum power required is at speeds of about 60 kts.

Stationary Flight

Power required in hover flight depends on gross weight, ambient conditions, and ground effect as well as on the wing flap position and the nacelle tilt angle. Figure 8 shows the hover power required versus gross weight.

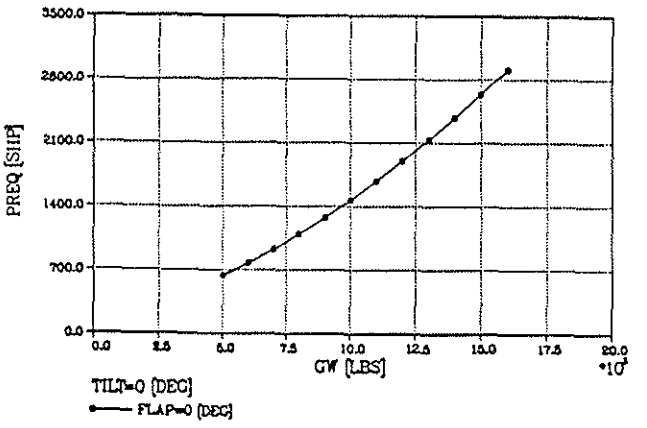

Figure 8 Hover Power Required versus Gross Weight

The data presented in this diagram are calculated for sea level (S.L.) and standard day (S.D.) conditions. These ambient conditions are used for all of the following performance and optimization results. The flap position and the nacelle tilt angle are 0 deg. The design gross weight for the XV-15 is 13000 lbs. According to Figure 8, the XV-15 theoretically has the capability to hover at a gross weight of 16000 lbs under the given standard ambient conditions. However, the maximum gross weight, which can be reached with maximum fuel, is about 15000 lbs. The engine power available with both engines operating is 3100 shp. Note that at the maximum gross weight, the XV-15 is not capable of hovering with only one engine operating.

Since the wing of the XV-15 is strongly influenced by the rotor wakes which cause a negative wing lift and thus virtually increases the gross weight in hover, the wing's flap position has a significant effect on hover power required. The negative wing lift in percentage of thrust is called wing download. As can be seen in Figure 9 the download decreases with increasing flap angle. The wing download in hover depends on the wing drag coefficients for angles of attack of about -90 deg.

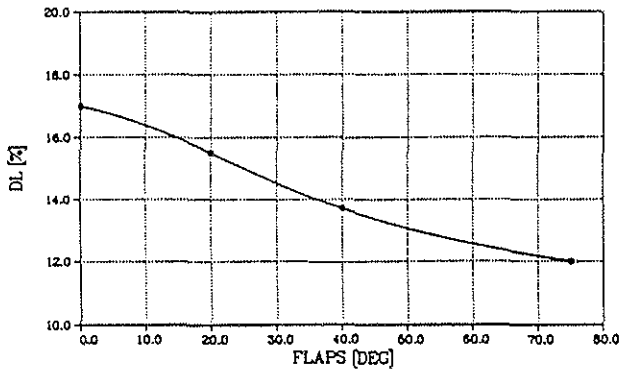

Figure 9 Wing Download versus Flap Position

Figure 10 shows the influence of the flap position on hover power required. The four standard flap positions are used for the calculations. At a gross weight of 15000 lbs, hover power required is reduced by more than 200 shp, if the flaps are deflected by 75 deg.

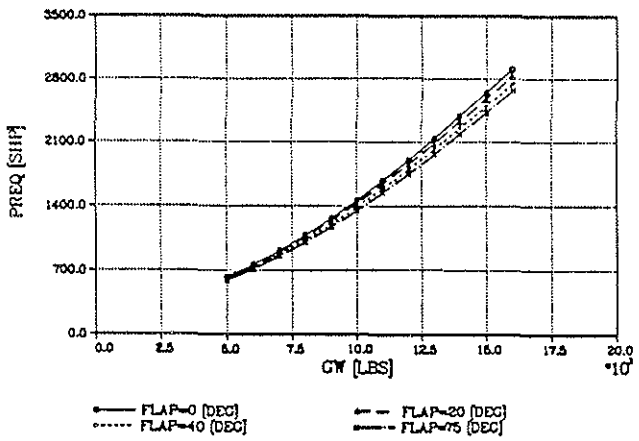

Figure 10 Hover Power Required versus Gross Weight, Tilt=0 deg

Figure 11 presents hover power required versus gross weight for varying tilt angles, but no flap deflection.

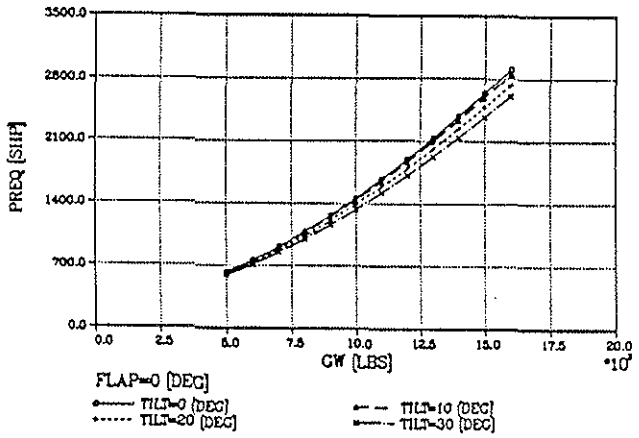

Figure 11 Hover Power Required versus Gross Weight, Flap=0 deg

Although the range of nacelle tilt angles used in hover flight is small, between -5 and 10 deg, the influence of the tilt angle on hover power required is shown for angles up to 30 deg. Because of the pitch attitude, tilt angles higher than 10 deg are normally not used in practice.

With increasing nacelle tilt the hover power required is decreasing due to the change in wing download. The influence of the nacelle tilt angle is reduced if the flaps are deflected.

As mentioned above, power required is influenced by the ground effect. The ground effect is mainly a reduction in induced power due to a reduced rotor-induced velocity. The induced velocity in the rotor disc area is reduced with decreasing rotor-ground distance. Since the wing download depends on the rotor induced velocity, a secondary effect in ground effect is a reduction in wing download.

Figure 12 gives the ratio of power coefficient IGE divided by the power coefficient OGE versus the non-dimensional rotor height, which is the rotor height above ground divided by the rotor diameter. For rotor heights greater than twice the rotor diameter, the ground effect can be neglected. A non-dimensional rotor height of H/D=0.52 is the lowest possible value for the XV-15. If the aircraft is on the ground, the rotor height above the ground is H=13 ft (no tilt angle).

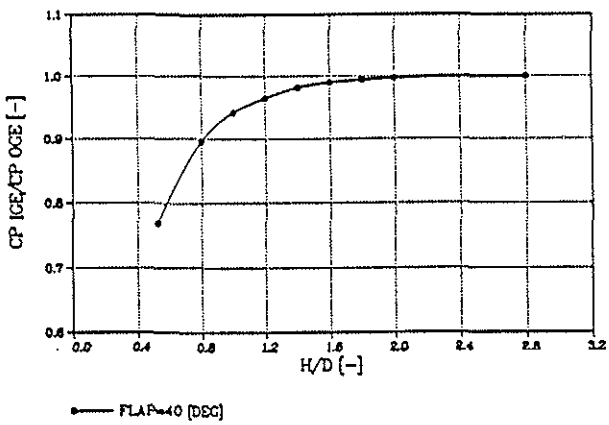

Figure 12 Power Coefficient Ratio versus Non-Dimensional Rotor Height IGE

The ground effect reduces the power required up to nearly 25 %, which is surprisingly high, since only a part of the rotor wakes interacts directly with the ground. Figure 13 shows the results for the ground effect in dimensional form, hover power

required OGE and IGE versus gross weight, for the minimum rotor height above ground. At a gross weight of 15000 lbs, the amount of reduction in power required is more than 600 shp.

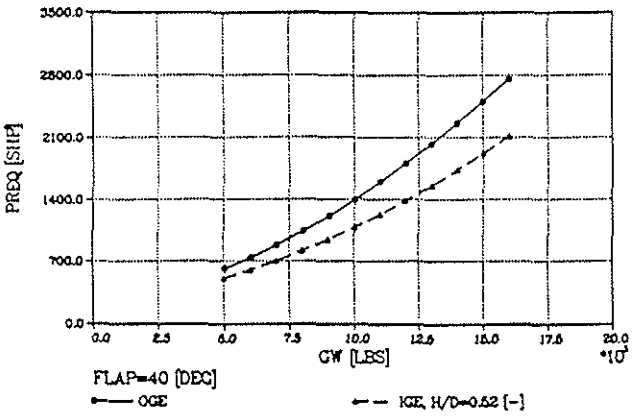

Figure 13 Hover Power Required OGE and IGE versus Gross Weight

Although the reduction in power required is considerable, the XV-15 at a weight of 15000 lbs does not have the capability to hover IGE, if one engine is inoperative.

As described in Section 3, the original GTRS delivered to Georgia Tech used an erroneous equation for the calculation of the rotor-induced velocity. After correcting the equation and modifying the profile drag coefficients for the rotor, as well as the wing-pylon drag coefficients, the power required in forward flight changed. Figure 14 presents power required versus forward speed for the original and the modified GTRS. Whereas the original GTRS model indicates a slight increase in power required for speeds between 0 and 10 kts, the modified GTRS model shows a decrease in power required starting from hover flight (V=0 kts). The small difference in hover power required is explained by a modified download.

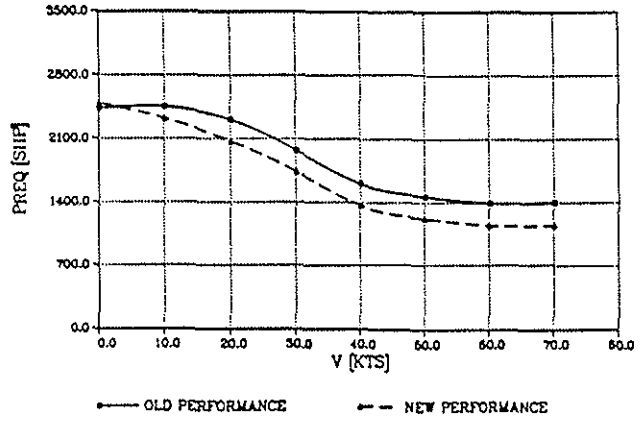

Figure 14 Power Required versus Forward Speed, Tilt=0 deg, Flap=40 deg

Power required changes in the entire forward flight regime. The new GTRS model was used for all calculations.

In forward flight the ground effect changes not only with rotor height above the ground but also with forward speed. The ground effect diminishes rapidly if forward speed increases. Figure 15 shows power required versus forward speed for forward flight OGE and IGE. For the rotor height, again the lowest possible value was chosen. This case is of interest for the short takeoff simulation, although the pitch angle in forward flight is of course different from the pitch angle during the rolling phase (pitch angle is 0 deg). The power required IGE is given for two different washout coefficients. The washout coefficient was reduced from -0.08 to -0.04 so that the ground effect diminishes less rapidly. Since the wing produces an additional ground effect this result seems to be more realistic. However, there are neither tilt rotor flight tests nor windtunnel investigations to confirm the predicted ground effect.

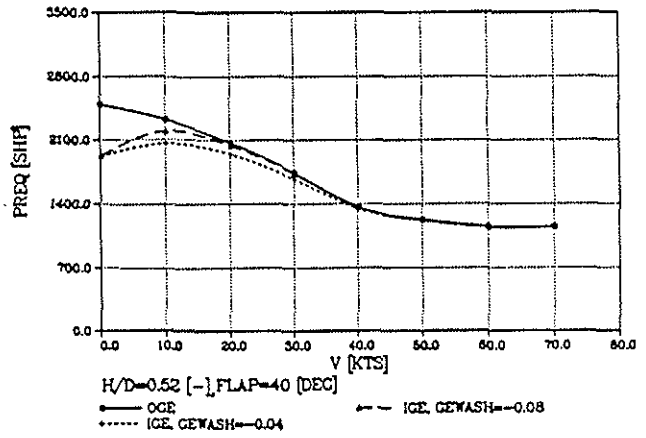

Figure 15 Power Required OGE and IGE versus Forward Speed, Tilt=0 deg

The influence of wing flap deflection and nacelle tilt angle on power required in forward flight is shown in Figures 16 and 17. The IGE condition is chosen. The non-dimensional rotor height is 0.52. The flap deflections are 40 and 75 deg. The tilt angle changes from 0 to 20 deg. Higher nacelle tilt angles are not flyable in the speed regime between 10 and 60 kts, since the wing stalls. For low speeds and a tilt angle greater than 25 deg the pitch attitude and thus the angle of attack in the area of the wing not influenced by the rotor wakes are too high. The high pitch angle is explained by the fact that in the low speed regime the parasite

drag is still relatively small, and the rotor thrust is mainly required to compensate for the weight. Therefore, the pitch angle is about the magnitude of the tilt angle.

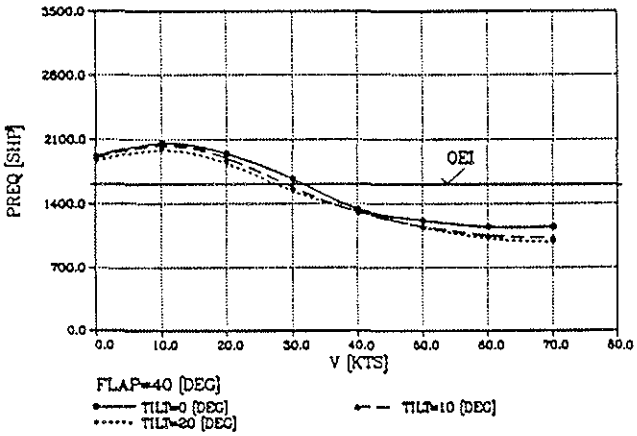

Figure 16 Power Required versus Forward Speed, Flap=40 deg, H/D=0.52

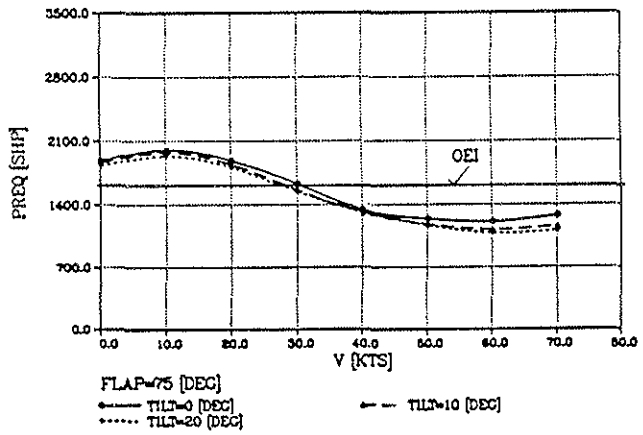

Figure 17 Power Required versus Forward Speed, Flap=75 deg, H/D=0.52

Power required is reduced with increasing tilt angle. Below the forward speed of 40 kts the decrease in power required per 10 deg tilt angle is less than 100 shp. Assuming a maximum contigency power of 1600 shp per engine, horizontal forward flight IGE with OEI is possible at about 30 to 35 kts. Horizontal forward flight OGE with OEI is possible at speeds of 35 kts and higher.

Ground Trim

Before starting the takeoff simulation, the aircraft must be trimmed on the ground. This can be performed using the methods as described in Ref. 24. Depending on the longitudinal cyclic pitch (50 % in this study) and the nacelle tilt angle, the collective control input is iteratively determined so that the maximum brake force is used. The collective control inputs required for the ground trim are in the range of 20 to 40 %. Figures 18 and 19 give the collective and the power required for varying tilt angles. The flap deflection is 40 deg. The flap deflection has only a small influence on the ground trim.

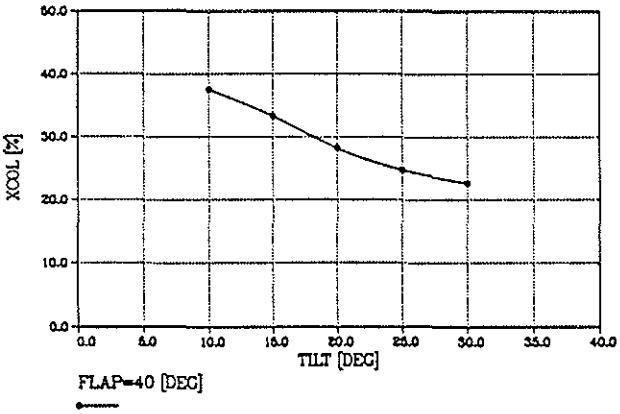

Figure 18 Collective Control Input versus Nacelle Tilt

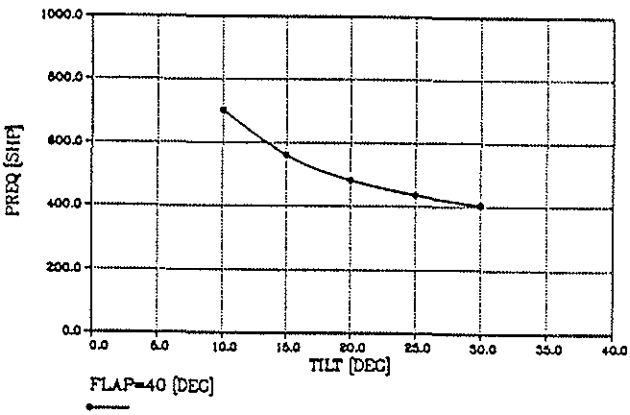

Figure 19 Power Required versus Nacelle Tilt

With increasing tilt angle, the collective control input must be decreased, mainly because the maximum brake force is reached. The maximum brake force depends on the vertical landing gear forces, since the friction between the wheels and the ground is the limiting factor. Figure 20 shows the vertical forces of the nose and the main gear as well as the maximum brake force versus the nacelle tilt angle. The maximum brake force is increasing with increasing tilt angle, because the vertical landing gear forces are increasing due to the decreasing vertical component of the rotor thrust.

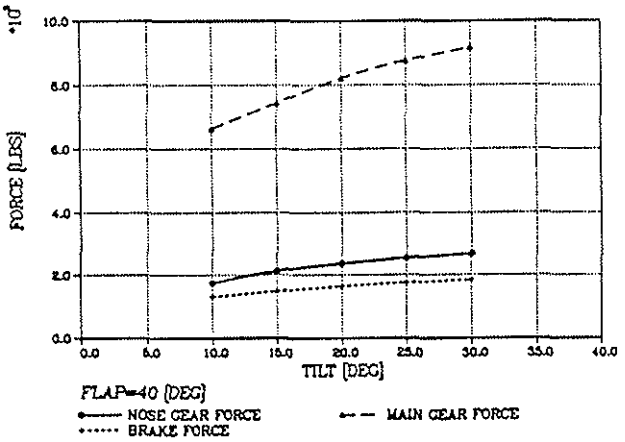

Figure 20 Landing Gear Forces versus Nacelle Tilt

Takeoff

The ground roll distance, i.e. the distance to accelerate the aircraft together with the distance to rotate the aircraft is the major part of the total takeoff distance, as has been shown in Figures 1 and 2. The speed V1 in Figure 1 is the takeoff decision speed. In the case that one engine fails before reaching V1, the pilot has to reject the takeoff. If one assumes, that a rejection of the takeoff after initiating the rotation can not be recommended because of safety reasons, the decision speed is always less or equal the speed VROT. The horizontal distance versus forward speed presented in the following sections are valid for the case, that the nose and the main gear still have ground contact and no rotation is initiated.

The acceleration distance depends on power required (gross weight, ambient conditions), and on power available. The influence of the gross weight is shown in Figure 21 for standard day and sea level conditions.

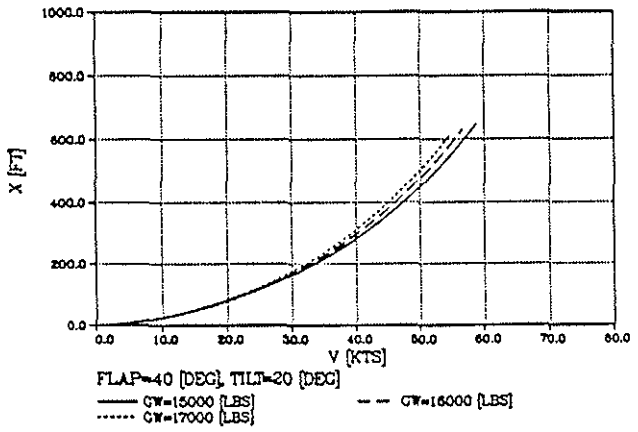

Figure 21 Acceleration Distance versus Speed, Influence of Gross Weight

The gross weight is varied from 15000 to the fictitious value of 17000 lbs. A comparable accerelation distance can be reached also for lower gross weights and more unfavourable ambient conditions. The acceleration distance increases with speed. The torque limit is 85000 in-lbs per rotor (equivalent to OEI power available of 1600 shp). The increase in distance with higher gross weights is relatively small. But one has to keep in mind that with increasing weight the lift-off speed increases, i.e. higher speeds have to be achieved during the acceleration.

The engine power available for the OEI condition is limited by the torque. If the torque limit is reduced, less engine power is available, and the acceleration distance increases, Figure 22. The torque given in the figure, is the mast torque per rotor.

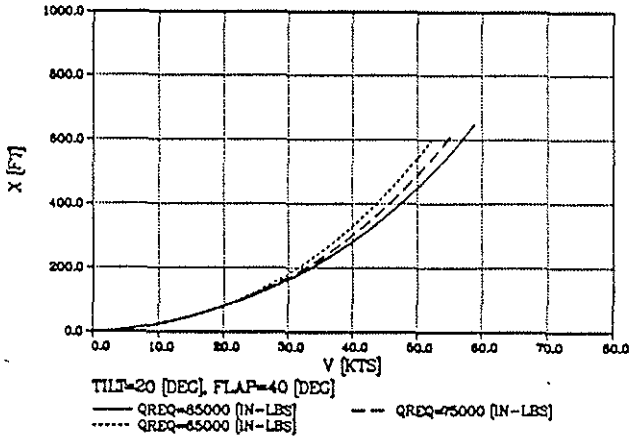

Figure 22 Acceleration Distance versus Speed, Influence of Torque Limit

In Figure 23, the same flap/tilt configuration is chosen. The gross weight is 15000 lbs and is also used for the following results. The longitudinal control input is 50 %.

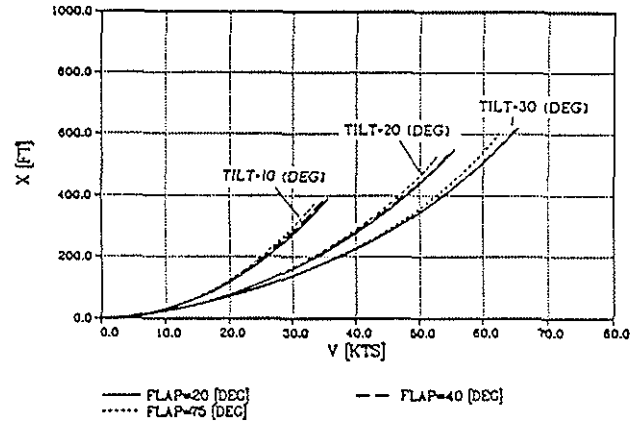

Figure 23 Acceleration Distance versus Speed, Tilt=20 deg

Figure 23 shows the acceleration distance for different flap deflections and nacelle tilt angles. The flap deflection is varied from 20 to 75 deg and the tilt angle from 10 to 30 deg. The torque per rotor is 85000 in-lbs.

The influence of the flap angle is small and is mainly due to higher wing drag coefficient with increasing flap angle. The nacelle tilt angle has far more influence. As the tilt angle increases, the thrust of the rotors is tilted further forward and can be used to accelerate the aircraft faster.

The simulation was terminated either when a speed of 65 kts was reached, or when the nose or the main gear lose ground contact.

Figures 24 to 26 show the vertical force of the nose and landing gear for the corresponding tilt angles.

In the case of a 30 deg tilt angle, Figure 23, the speed of about 65 kts was reached for all flap angles. The vertical forces at a speed of 65 kts, Figure 24, are considerable and the aircraft would not takeoff without rotation initiated by the pilot.

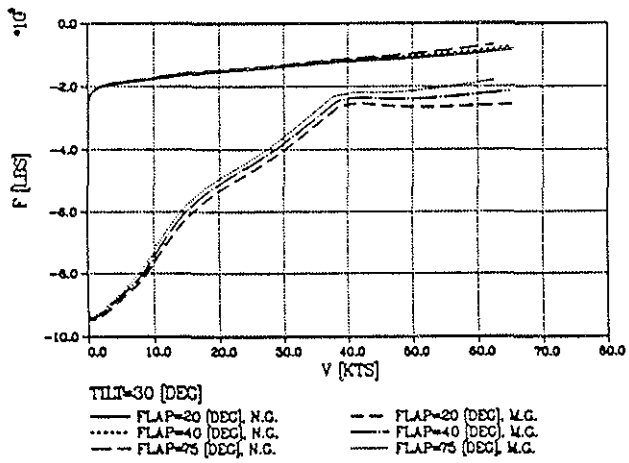

Figure 24 Vertical Force of Nose and Main Gear versus Speed, Tilt=30 deg

This is not the case for tilt angles of 10 and 20 deg, Figures 25 and 26. Especially for a tilt angle of 10 deg, the main gear vertical force reaches a zero value before the nose gear vertical force (i.e., the main gear has no ground contact at speeds of about 33 kts). Therefore, the pilot would have to rotate the aircraft before reaching this speed. A rotation over the nose gear has to be excluded for different reasons, e.g. structural limitations.

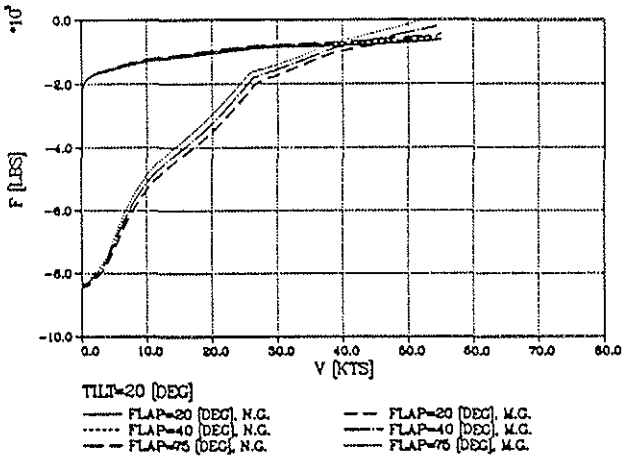

Figure 25 Vertical Force of Nose and Main Gear versus Speed, Tilt=10 deg

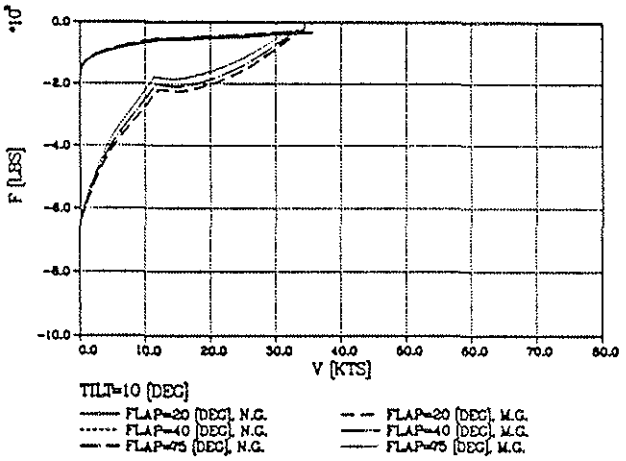

Figure 26 Vertical Force of Nose and Main Gear versus Speed, Tilt=10 deg

The longitudinal control setting during the acceleration phase, which influences the pitch moment, has an effect on the vertical gear forces. In the case of 10 and 20 deg tilt angles, a less forward longitudinal stick position would be required in order to achieve higher speeds, before the main gear looses ground contact. A minimum speed has to be obtained, at which a climb capability OGE for the given power available is assured.

For a takeoff with a nacelle tilt of 10 deg, Figure 23, the critical speeds are of the magnitude of the minimum speed required to attain at least horizontal flight capability OGE, see also Figures 16 and 17. For a takeoff with a nacelle tilt of 20 deg the speeds of about 50 kts are sufficiently above the minimum speed for horizontal flight.

These results will be helpful for the interpretation of the optimization results.

5. Optimization Results

The optimization results are obtained using a given wing flap deflection and a given nacelle tilt angle. The longitudinal control input, the rotation speed, and the final speed for the climb phase are allowed to vary during the optimization. The optimizer has the task of finding the optimal longitudinal input and the optimal rotation speed, which minimizes the takeoff distance. A low rotation speed gives a short acceleration distance. A high rotation speed close to the speed for minimum power required yields more excess power for the climb phase. For all optimization runs the OEI case is chosen, i.e. the torque per rotor is 85000 in-lbs. Variations of speed, longitudinal control input, and height with horizontal distance are presented in Figure 27 for the optimal takeoff with a nacelle tilt angle of 10 deg and a wing flap deflection of 40 deg.

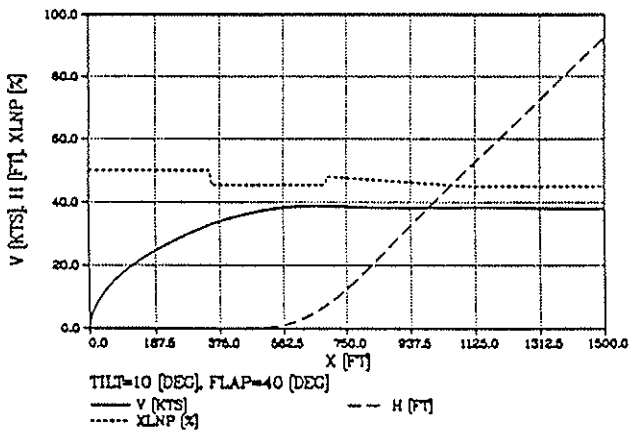

Figure 27 Optimized Takeoff with Tilt=10 deg, Flap=40 deg

The rotation is initiated at a speed of 33 kts. The distance to this point is 351 ft. The speed at lift-off is 36.5 kts, and the distance for lift-off is 463 ft. The takeoff distance to clear the 35 ft height is 959 ft. The final speed during the climb is 38 ft. For a nacelle tilt of 10 deg, the range for potential rotation speeds is small. The minimum speed required for horizontal flight at the given OEI power available is about 28 kts, see Figure 16. The maximum speed is about 35 kts, because the main gear loses ground contact before the nose gear becomes free, Figure 26. The longitudinal control input of 50 % remains fixed during the rolling phase. The speed for the climb phase is far below the speed for best climb angle, which is about 55 kts. The speed for best climb angle can be estimated by drawing a tangent from point V=0 kts, P=1600shp to the power required curve, Figure 16. The tangent point at the power curve yields the speed for best climb angle.

Figure 28 presents the optimized takeoff for a wing flap deflection of 75 deg. The tilt angle is the same as in Figure 27.

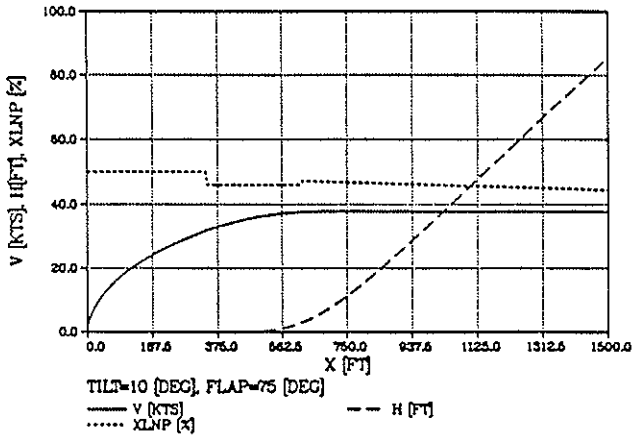

Figure 28 Optimized Takeoff with Tilt=deg, Flap=75 deg

The takeoff distance is 1002 ft. The reason for this increase in takeoff distance is not obvious, and is not due to a longer acceleration distance, as one would except. The rotation speed, the liftoff speed, and the acceleration distance are about the same for both cases. The transient speeds after lift-off and the final speeds are slightly different. For the 40 deg flap angle case, the speed shows a small overshoot beyond the final value. During this phase, the climb rate is higher than in the 75 deg flap angle case. In addition, a slightly higher final speed gives a better climb angle for the 40 deg flap configuration. However, the differences are small.

The next two figures show the optimized takeoff for a nacelle tilt angle of 20 deg. Figure 29 presents a takeoff with a wing flap deflection of 40 deg, while Figure 30 shows a takeoff with a flap deflection of 75 deg.

Evaluation of Figures 29 and 30 gives the following results (values in brackets are for the flap angle of 75 deg): The rotation speeds are 38 kts (40 kts), and the acceleration distances are 252 ft (287 ft). The aircraft is airborne at 370 ft and 42 kts for both flap configurations. The 35 ft height

is cleared after 706 ft (744 ft) and the final speeds during the climb phase are 40 kts (42 kts). The speeds are constant after the aircraft reaches the 35 ft height. Once again, a flap angle of 40 deg is more advantageous. For the 40 deg flap case, a shorter takeoff distance is reached by simply reducing the speed from 42 kts to 40 kts during the rotation phase. The final climb angle in both cases is the same.

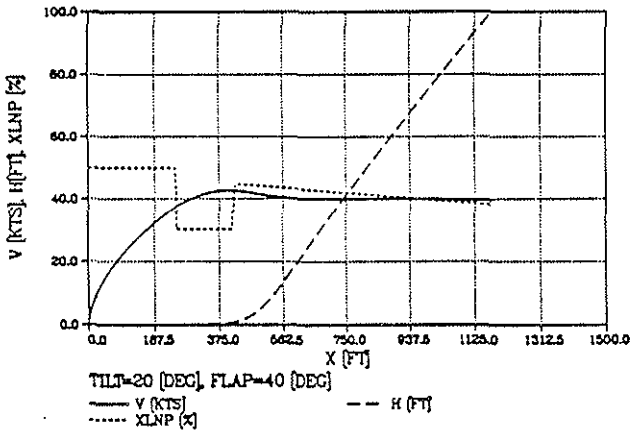

Figure 29 Optimized Takeoff with Tilt=20 deg, Flap=40 deg

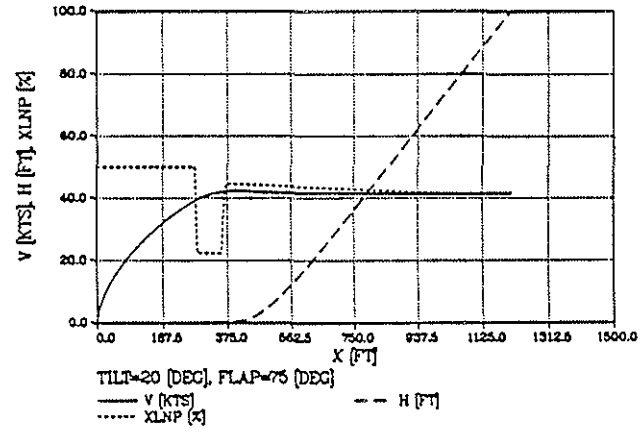

Figure 30 Optimized Takeoff with Tilt=20 deg, Flap=75 deg

The takeoff distances for a nacelle tilt angle of 20 deg are considerably shorter than the takeoff distances for a tilt angle of 10 deg, since more of the rotor thrust is used to accelerate the aircraft. Although the minimum speed required for horizontal flight is lower for a tilt angle of 20 deg compared to the minimum speed for the 10 deg case, see Figure 16, the optimizer chooses a higher rotation speed in order to take advantage of the higher excess power, i.e., higher climb rates, at higher speeds. The acceleration on the ground for a tilt angle of 20 deg can be carried out up to a rotation speed this high. The maximum speed, where the main gear clears the ground, is greater than 50 kts, see Figure 25.

Acceleration, while the aircraft is on the ground, is advantageous for two reasons. First, the favorable ground effect is utilized. Second, the takeoff procedure is easier to perform. An additional horizontal acceleration after lift-off would be of interest only for the takeoff with a 10 deg tilt angle where the aircraft is airborne at relative low lift-off speeds. However, negative pitch angles would be required, in order to achieve similar accelerations as for a nacelle tilt of 20 deg. The rotation of the aircraft to a negative pitch attitude after lift-off is rather unusual compared to takeoff procedures of fixed wing aircraft. For helicopters, similar maneuvers are used for the so-called running takeoff. During this maneuver, the helicopter is accelerated parallel to the ground using negative pitch angles.

If these maneuvers are excluded for a civil tilt rotor aircraft, the takeoff with 20 deg tilt angle is of clear advantage. Since a high acceleration capability is important, a further increase of the nacelle tilt angle could be advantageous. Therefore, a nacelle tilt angle of 30 deg was investigated. Figures 31 and 32 show the optimized takeoff maneuvers for a 30 deg tilt angle. Wing flap deflections of 40 and 75 deg are used.

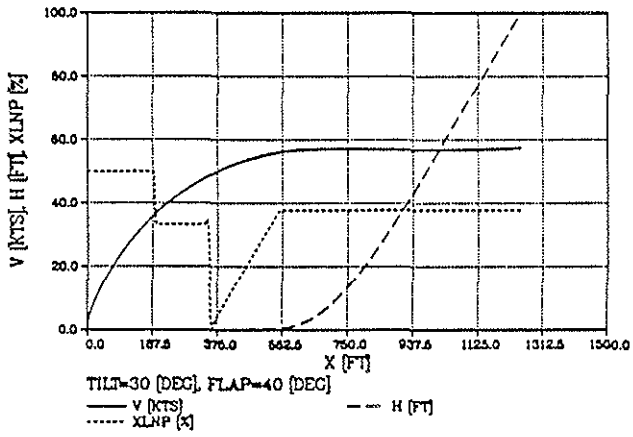

Figure 31 Optimized Takeoff with Tilt=30 deg, Flap=40 deg

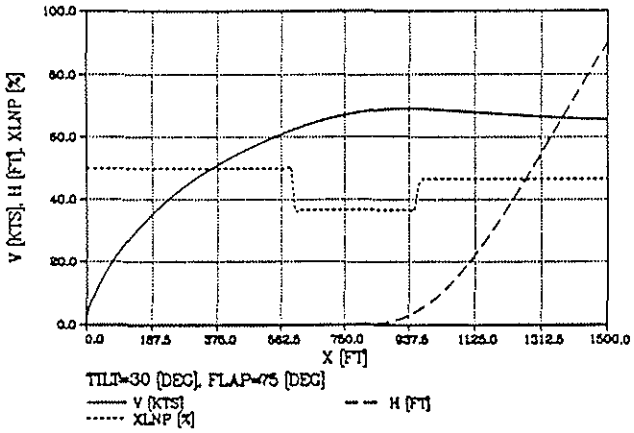

Figure 32 Optimized Takeoff with Tilt=30 deg, Flap=75 deg

The results in detail are (values for flap angle of 75 deg in brackets): The rotation of the aircraft starts at speeds of 36 kts (63 kts) after reaching a distance of 197 ft (602 ft). The lift-off speeds are 56 kts (68 kts) at the lift-off distances of 526 ft (801 ft). The 35 ft height is cleared after 898 ft (1204 ft), and the final speeds for the climb are 58 kts (65 kts).

The main limitation for takeoff at a nacelle angle of 30 deg is the wing angle of attack. It has already been mentioned in Section 4 that for this tilt angle, level flight below 60 kts is not possible because of wing stall. The limiting forward speed where the wing stalls varies with climb rate and cannot be determined easily. The optimization shows that the minimum forward speed required to rotate the aircraft and to climb without wing stall is still relative high. In the case of takeoff with 40 deg flap deflection, the longitudinal control changes in two steps. The first control input at low speed is too small to rotate the aircraft. Rotation at this point would lead to wing stall. The second control input at higher speeds uses the maximum allowable range. In the case of takeoff with 75 deg flap angle, the longitudinal control input is simpler. However, the required takeoff distance is considerably longer.

In general it can be stated that takeoff with a nacelle tilt angle of 30 deg requires higher rotation and higher lift-off speeds due to wing stall limitations. Higher rotation speeds and higher lift-off speeds lead to longer takeoff distances. A flap deflection of 40 deg is in all cases of advantage compared to the 75 deg flap deflection, although the differences in takeoff distance are small. The takeoff with a nacelle tilt angle of 20 deg and a wing flap deflection of 40 deg yields the shortest takeoff distance.

Before continuing the optimization with two additional parameters, nacelle tilt angle and wing flap deflection, only the nacelle tilt was included as parameter into the optimization process. However, these optimizations did not result in takeoff maneuvers, which were substantially different from the previous optimized takeoff maneuvers with a given nacelle tilt angle and given flap deflection. Although different initial conditions were chosen, the nacelle tilt angle changed only slightly. Considerable shorter takeoff were not obtained. The configuration, wing flap deflection 40 deg and nacelle tilt angle 20 deg, turned out to be a favorable configuration. This confirms the configuration selected by NASA for the XV-15 short takeoff flight tests. It is known to the author that NASA did some piloted simulations on the VMS at NASA Ames to gain experience in performing short takeoff maneuvers with the XV-15. These simulations have been carried out prior to the flight testing. However, no report about this simulation study exists.

6. Comparison with Flight Tests

Since the short takeoff flight tests are performed for one configuration, a nacelle tilt of 20 deg and a flap deflection of 40 deg, only the optimal takeoff from Figure 29 can be compared with test data. Figure 33 shows the takeoff distances from flight tests versus lift-off speeds (same figure as Figure 2).

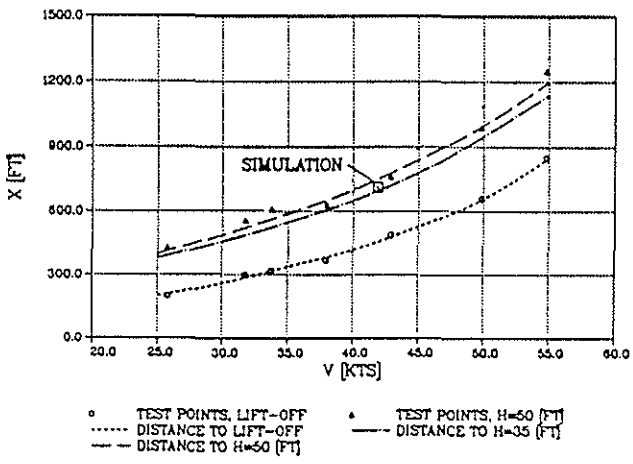

Figure 33 Takeoff Distance versus Lift-off speed

The simulated lift-off speed for this configuration is 42 kts and the final speed during the climb is 40 kts. The simulation result is shown in the diagram at a speed of 42 kts. It has to be noted that the airspeed measurement during the flight tests was not very accurate. Also, the speed varies during the climb. Therefore, a speed range could rather be chosen instead of one specific speed value.

The calculated takeoff distance is within the scattering of the flight tests. However, the simulated takeoff is an optimal takeoff giving the shortest takeoff distance. As can be seen in Figure 33, the XV-15 is capable of performing the takeoff at lift-off speeds down to 25 kts, i.e., considerable shorter takeoff distances can be reached. The takeoff at lift-off speeds of 25 kts could not be achieved by the simulation. A simple consideration yields that simulated takeoffs at these low speeds can not be carried out. Figure 16 shows that for the given OEI power available the level flight OGE can be performed at about 30 kts. A forward climb with climb rates of about 10 ft/sec, similar to climb rates of the flight tests, is only possible at even higher speeds of the magnitude of 35 kts. It appears that the GTR simulation has still deficiencies in calculating power required OGE in the low speed regime. Although the modifications, already made to the code, considerably reduced the power required in forward flight, the calculated power is still too high.

7. Conclusions

A simulation study was conducted to evaluate the short takeoff capabilities of the XV-15 tilt rotor aircraft. Different takeoff configurations with varying nacelle tilt angle and wing flap deflection were investigated using the generic tilt rotor simulation (GTRS). An optimization of the takeoff was performed minimizing the required takeoff distance.

First, the takeoff related performance in the low forward speed regime was investigated. After discovering deficiencies in the performance calculation of GTRS and correcting the calculation of the rotor-induced velocity, the power required for forward flight changed considerably. To match hover power required from flight tests, new profile drag coefficients for the rotor blades were estimated. In addition, the wing-pylon drag coefficients had to be changed to obtain a reasonable download in hover flight. Since no flight test data were available for low forward speeds, the accuracy of the performance calculation could not directly be determined. However, the comparison of simulated takeoff maneuvers with takeoff maneuvers from flight tests showed that calculated power required is still overpredicted.

Although the calculated performance of GTRS might not represent the XV-15 performance in the low speed regime with high accuracy, the simulation takes into account the major aerodynamic effects that influence the power required of a typical tilt rotor aircraft. The variation of calculated power required with parameters, such as gross weight, forward speed, IGE conditions, wing flap deflection, and nacelle tilt angle was presented.

Second, the optimization of a short takeoff maneuver was performed. It turned out that a takeoff with a nacelle angle of about 20 deg and a flap deflection of 40 deg yields the shortest takeoff distance. Takeoffs with a nacelle tilt of 10 deg and a nacelle tilt of 30 deg require considerably higher takeoff distances because of different reasons. The 10 deg tilt case yields long acceleration distances, since only a small part of the rotor thrust is used to accelerate the aircraft. The horizontal accelerations in the 30 deg tilt case are higher, but the aircraft has to be accelerated to higher speeds in order to not violate limitations imposed by wing stall.

The influence of the flap deflection on the takeoff distance is small. A flap deflection of 40 deg is advantageous compared to a flap deflection of 75 deg. The calculated takeoff distance at a lift-off speed of about 40 kts is in the range of the takeoff distances observed in flight tests. A takeoff at lift-off speeds of 25 kts could not be achieved by the simulated takeoff maneuvers. As already mentioned, the reason is the calculation of power required OGE, which is still to high.

The most important requirement for the simulation of takeoff maneuvers is the reliable calculation of power required and power available. The GTRS model has still deficiencies in calculating power required in the low forward flight regime. Therefore, further improvement of GTRS in this area should be the next major step before using the code for continuing takeoff studies. Bell and NASA are planning flight tests in the low speed flight

regime. These tests were initiated by Sam Ferguson, after he was informed about the results of GTRS for low speeds. Additional flight test data will be very helpful in improving the performance calculation of GTRS.

When a reliable performance calculation in the low speed regime is achieved, it is recommended to reevaluate the short takeoff procedure using a piloted simulation. The main advantage of the piloted simulation is that the experience of test pilots can be used to find optimal takeoff maneuvers faster. In addition, the human behavior can be incorporated in this study. This way, optimal takeoff procedures can be found, which take also into account the pilot workload. Furthermore, the real environment, such as terminal conditions etc., can be included in the simulation task.

References

1. E.E. Blount, Airplane-Helciopter, United States Patent 1 951 817, March 20, 1934

2. M.D. Maisel, Tilt Rotor Research Aircraft Familiarization Document, NASA TM X-62, 407, January 1975

3. W.L. Arrington et. al., XV-15 Tilt Rotor Research Aircraft Flight Test Data Report, Vol. 1 to 5, NASA CR 177406, June 1985

4. S. Martin Jr., R. Ostlund, V-22 Development Status, 15th European Rotorcraft Forum, Amsterdam, September 1989

5. Civil Tilt Rotor Missions and Applications: A Research Study, Boeing Commercial Airplane Company, Renton WA, NASA CR 177452, Summary Final Report, July 1987

6. J.B. Wilkerson, R.S. Taylor, Civil Tiltrotor Aircraft: A Comparison of Five Candidate Designs, 44th Annual Forum of the American Helicopter Society, Washington D.C. June 1988

7. B. Gmelin et. al., Preliminary Comparisons of Tilt Rotor and Compound Helicopter for Civil Applications, 45th Annual Forum of the American Helicopter Society, Boston, May 1989

8. W. Muggli, R.D. von Reth, H. Huber, EUROFAR-Europäisches Projekt für ein senkrecht startendes Verkehrsflugzeug, Jahrestagung der Deutschen Gesellschaft für Luft- und Raumfahrttechnik, Darmstadt, Oktober 1989

9. J.M. Drees, Expanding Tilt Rotor Capabilities, Vertica Vol. 12, No. 1/2, pp. 55-67, 1988

10. T.K. Flemming et. al., Creating a Commercial Tilt Rotor (CTR) System, 45th Annual Forum of the American Helicopter Society, Boston, May 1989

11. J.A. Weiberg, D.C. Dugan, M.R. Gerdes, XV-15 N703 Takeoff Performance, NASA Memo FHT: 237-5/4554, September 1982

12. Interim Airworthiness Criteria, Powered-Lift Transport Category Aircraft, Department of Transportation, Federal Aviation Administration, Forth Worth, July 1988

13. H.G. Jacob, An Engineering Optimization Method with Application to STOL-Aircraft Approach and Landing Trajectories, NASA TN D-6978, September 1972

14. H.G. Jacob, Rechnergestütze Optimierung statischer und dynamischer Systeme, Springer Verlag, Berlin, 1982

15. G.D. Hanson, S.W. Ferguson, Generic Tilt Rotor Simulation (GTRSIM) User's and Programmer's Guide, Vol.1 and 2, NASA CR-166535, October 1983, Rev. A, September 1988

16. S.W. Ferguson, A Mathematical Model for Real Time Flight Simulation of a Generic Tilt Rotor Aircraft, NASA CR-166536, October 1983, Rev. A. September 1988

17. XV-15 Flight Manual, Bell Helicopters Textron, TP-78-XV-1, August 1980

18. S.W. Ferguson, Development and Validation of Simulation for a Generic Tilt Rotor Aifrcraft, NASA CR-166537, April 1989

19. A. Gessow, A. Crim, An Extension of Lifting Rotor Theory to Cover Operation at Large Angles of Attack and High Inflow Conditions, NACA TN 2665, 1952

20. W. Castles Jr., N. New, A Blade Element Analysis for Lifting Rotors that is Applicable for Large Inflow and Blade Angles and any Reasonable Blade Geometry, NACA TN 2656, July, 1952

21. J.M. Drees, A Theory of Airflow Through Rotors and its Application to some Helicopter Problems, The Journal of the Helicopter Association of Great Britain, Vol.3, No.2, September 1949

22. J.S. Hayden, The Effect of the Ground on Helicopter Hovering Power Required, 32nd Annual Forum of the American Helicopter Society, Washington D.C., May 1976

23. T. Cerbe, G. Reichert, H.C. Curtiss Jr., Influence of Ground Effect on Helicopter Takeoff and Landing Performance, 14th European Rotorcraft Forum, Milano, 1988

24. T. Cerbe, Short Takeoff Optimization for the XV-15 Tilt Rotor Aircraft, Final Report, Georgia Institute of Technology, April 1990

Acknowledgements

Special thanks go to Mr. Cliff McKeithan of the Georgia Institute of Technology and Mr. Sam Ferguson of Systems Technology Incorporation. Their experience with the XV-15 and the GTRS model was of great help for this study.

The research was funded for a one year period by a postdoctoral scholarship of the Deutsche Forschungsgemeinschaft, Bonn, Germany.